

This paper was originally published as an *ASHRAE Research Journal - Science and Technology for the Built Environment* and may be cited as:

Mohammadamin Ahmadfard & Michel Bernier (2018) Modifications to ASHRAE's sizing method for vertical ground heat exchangers, *Science and Technology for the Built Environment*, 24:7, 803-817, DOI: 10.1080/23744731.2018.1423816

©ASHRAE www.ashrae.org. *Science and Technology for the Built Environment*, 24:7, 803-817, 2018.



Modifications to ASHRAE's sizing method for vertical ground heat exchangers

Mohammadamin Ahmadfard & Michel Bernier

To cite this article: Mohammadamin Ahmadfard & Michel Bernier (2018) Modifications to ASHRAE's sizing method for vertical ground heat exchangers, Science and Technology for the Built Environment, 24:7, 803-817, DOI: [10.1080/23744731.2018.1423816](https://doi.org/10.1080/23744731.2018.1423816)

To link to this article: <https://doi.org/10.1080/23744731.2018.1423816>



Accepted author version posted online: 22 Jan 2018.
Published online: 29 Jan 2018.



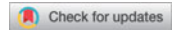
Submit your article to this journal [↗](#)



Article views: 114



View Crossmark data [↗](#)



Modifications to ASHRAE's sizing method for vertical ground heat exchangers

MOHAMMADAMIN AHMADFARD and MICHEL BERNIER*

Department of Mechanical Engineering, Polytechnique Montréal, C.P. 6079, Succ. Centre-ville, Montréal H3T 1J4, Canada

The current article proposes modifications to the ASHRAE sizing equation for vertical ground heat exchangers. The proposed method uses the same three pulse approach as the current sizing equation but uses g-functions to calculate the effective ground thermal resistances. One key feature of the iterative methodology is the ability to calculate new g-functions as the geometry morphs during the solution process. Long-term g-functions are evaluated analytically using the finite line source (FLS) solution over borehole segments while so-called short-term g-functions are calculated based on a hybrid analytical/numerical method to account for the borehole thermal capacity. The current article examines three aspects of the proposed methodology. First, it is shown that the time-consuming evaluation of the full g-function curve, typically obtained by temporal superposition, is not necessarily required. Second, the optimum number of borehole segments to obtain an accurate bore field length with reasonable calculation time is examined. The selection of a convergence criteria and its impact on calculation time is also discussed. The excellent agreement between results obtained with the proposed alternative method and the ones obtained from other design software tools confirms the validity of the proposed method. Finally, it is shown that short-term effects can have a relatively significant effect on the calculation of the required borehole length.

Introduction

Accurate sizing of vertical ground heat exchangers (GHEs) for ground source heat pump (GSHP) systems is important to limit drilling costs and avoid operational problems. A typical GSHP system is presented schematically in Figure 1 where a fluid loop links a series of heat pumps to six boreholes (in a 3×2 configuration). In this figure, D is the borehole buried depth, H is the borehole length, B is the borehole spacing, r_b is the boreholes radius, r_p is the pipe radius of the U-tube pipes and d_p is the center-to-center pipe distance. The important ground properties are the temperature T_g , the thermal conductivity k_g , and the thermal diffusivity, α_g .

As shown in Figure 1, GHEs are usually piped in parallel and it is generally assumed that the total flow rate is divided equally among all boreholes and that each borehole has the same inlet temperature. The heat pump inlet temperature,

$T_{in, hp}$, is the average of the outlet temperatures of all boreholes. This temperature must remain within limits set by heat pump manufacturers. The lower limit for the inlet temperature, T_L , can be as low as $\approx -5^\circ\text{C}$ while the high temperature limit T_H can reach $\approx 45^\circ\text{C}$.

Equation-based design methods (ASHRAE Handbook 1995; Bose et al. 1985) and simulation-based design methods (Hellström and Sanner 2000; Spitler 2000) can be used to size boreholes. Spitler and Bernier (2016) have categorized these methodologies into five levels (0 to 4) with increasing complexities and accuracy. Level 0 are rules-of-thumb sizing methods, level 1 and 2 cover the equation based models that use one or three ground load pulses while level 3 and 4 are simulation based sizing models that use monthly or annual hourly ground loads. Most of these models use a derivative of Equation 1 for determination of the boreholes length.

$$L = \frac{\sum_{i=1}^N q_i R_i + q_h R_b}{T_m - (T_g + T_p)}, \quad (1)$$

where L ($= N_b \times H$, N_b is the number of boreholes) is the total required borehole length, q_i is a ground thermal pulse associated with a certain time period, R_i is the corresponding effective ground thermal resistance, q_h is the peak ground

Received April 16, 2017; accepted December 18, 2017

Mohammadamin Ahmadvard is Student Member ASHRAE and a PhD student. Michel Bernier, PE, PhD is Fellow ASHRAE and a Professor.

*Corresponding author e-mail: michel.bernier@polymtl.ca

Color versions of one or more of the figures in the article can be found online at www.tandfonline.com/uhvc.

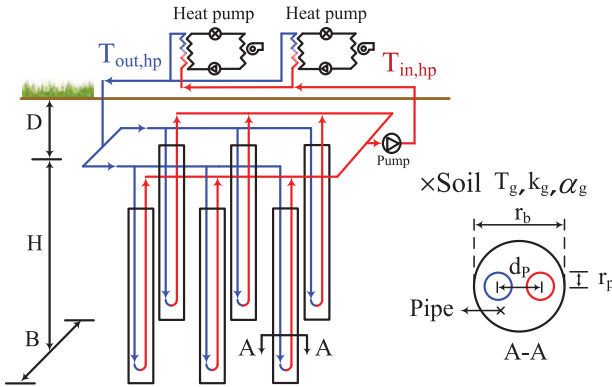


Fig. 1. Schematic illustration of a typical GSHP system.

thermal pulse, R_b is the effective steady-state borehole thermal resistance, T_m is the mean borehole fluid temperature ($= (T_{inHP} + T_{outHP})/2$), and T_p is a temperature penalty to account for the ground temperature increase (or decrease) caused by borehole-to-borehole thermal interaction when the annual ground load imbalance is important. This equation can be used by one pulse (level 1), three pulses (level 2), monthly pulses (level 3), and hourly pulses (level 4) and can be solved directly or iteratively when values of R_i depend on L . By increasing the number of load pulses the accuracy of the sizing model increases at the expense of increased mathematical complexity and calculation time. Among these models, the ASHRAE sizing equation, a level 2 method, is a good compromise between accuracy and calculation time.

The original ASHRAE sizing method, which is based on the work of Kavanaugh (1995), first appeared in the ASHRAE Handbook (1995). The original format of this equation has been reformatted by Bernier (2006) and is presented in Equation 2. This equation will be referred to as the ASHRAE classic sizing equation.

$$L = \frac{q_a R_{ga} + q_m R_{gm} + q_h R_{gh} + q_h R_b}{T_m - (T_g + T_p)} \quad (2)$$

The summation term includes three thermal pulses and their corresponding effective ground thermal resistances. The time periods of the three thermal pulses, q_a , q_m , and q_h are typically 10 years, 1 month, and 4 hours (or 6 hours in certain cases), respectively. The corresponding effective ground thermal resistances, R_{ga} , R_{gm} , and R_{gd} are calculated using the infinite one-dimensional (1D; radial) cylindrical heat source (ICS) analytical solution and they do not depend on borehole length. Borehole-to-borehole thermal interaction is accounted for using the temperature penalty term in the denominator. The main advantage of the ASHRAE sizing equation is that it can be solved directly and it does not require an iterative solution procedure when tabulated values of T_p are used directly. However, if T_p needs to be calculated for a specific geometry, then Equation 2 needs to be solved iteratively as T_p depends on the borehole length. It should be noted that if the annual ground load is balanced (i.e., $q_a = 0$), the calculations of T_p and R_{ga} are irrelevant and the ICS solution is adequate for sizing purposes. Despite its

simplicity, several authors have noted important deficiencies in the ASHRAE sizing equation:

1. The ICS used for evaluating the ground thermal resistances neglects axial heat transfer.
2. The temperature penalty calculation is inaccurate.
3. It does not size the length correctly if the maximum length is required in the first year of operation.
4. It does not account for short-term effects associated with borehole thermal capacity.
5. The value of the steady-state borehole thermal resistance does not account for the impact of the vertical temperature variation of the fluid inside the U-shaped tubes.

In the following paragraphs, solutions to these issues proposed by various authors are reviewed and then the proposed model is described.

Philippe et al. (2009) focused on the first deficiency. They determined the impact of neglecting the axial effects on the three ground thermal resistances. Their analysis showed that the 10-year effective ground thermal resistance, R_{ga} , is the most affected and as noted by Spitzer and Bernier (2016), the weight of R_{ga} in Equation 2 determines whether it has a significant impact on L or not.

The second drawback is much more important. It concerns the determination of the temperature penalty (T_p in Equation 2) which is suggested to be evaluated based on a rudimentary table of values on a limited number of configurations (ASHRAE 2015). This has motivated researchers Bernier et al. (2008), Fossa (2011), Fossa and Rolando (2013) and Capozza et al. (2012) to introduce various methodologies based on a more rigorous evaluation of the temperature penalty.

Bernier et al. (2008) evaluated T_p based on the difference between the g-function for a specific bore field with N_b boreholes, g_{Nb} , and the g-function of a single borehole, g_1 . They proposed a correlation that evaluates the temperature penalty of equally spaced rectangular bore fields which is within $\pm 10\%$ of the exact values, when $g_{Nb} - g_1 > 15$. Their results show that the ASHRAE equation can underestimate the value of T_p significantly. This methodology was used by Philippe et al. (2010) in a simple spreadsheet tool to obtain the length of single boreholes and rectangular bore fields. Since the temperature penalties depend on borehole length, which is unknown *a priori*, iterations are required.

Fossa (2011) has proposed a different definition for T_p . He has defined a “true or reference” temperature penalty to correct the error introduced by the use of the ICS solution when compared to the g-function of the bore field under consideration. Therefore, the temperature penalty of a single borehole is not zero as was the case in the study by Bernier et al. (2008). Fossa and Rolando (2013, 2015, 2016) have suggested a correlated equation (called Tp8) which examines the influence of eight surrounding boreholes. They have reported that the ASHRAE equation typically underestimates the “true” temperature penalty values by more than 40% (Fossa and Rolando 2015). The lengths evaluated based on the temperature penalties obtained from the ASHRAE equation have errors ranging from 17% to 50% while the ones evaluated with their proposed correlated equation have an average error

of 3% with respect to reference values (Fossa and Rolando 2015). Finally, they showed that the correlation suggested by Bernier et al. (2008) has a difference of less than 6% with their reference method for the rectangular and square bore fields.

Monzó et al. (2016) focused on the second and the third weak points of the classic ASHRAE sizing equation. They proposed to use the same three-pulse technique used in the ASHRAE sizing method with two modifications. First, the yearly ground load is replaced by the average ground load of the previous months. Second, the temperature penalty, T_p , is based on the average ground load of the previous months and is evaluated using g-functions. The methodology involves a three-step process. First, ground loads need to be analyzed and properly ordered. Then, using these loads, and assuming a temperature penalty $T_p = 0$, a first set of required lengths is determined for each month. Finally, an iterative process is initiated to account for the temperature penalty in each month to obtain the final required length for the worst condition. Monzó et al. (2016) have shown that the starting month can have a significant impact on the design length equation. Their proposed method compares favorably well with a commercial software tool.

Short-term effects have been analyzed by several authors and a complete literature review on the subject has been presented by Li and Lai (2015). Yavuzturk and Spitler (1999) were among the first to evaluate these effects. They used a two-dimensional (2D) finite volume method and calculated short-term g-functions. Others (Pasquier and Marcotte 2012; Ruiz-Calvo et al. 2015; Zarrella et al. 2011) have used thermal resistance-capacity (TRC) networks to study these effects. This problem can also be solved by simplifying the geometry in the borehole with an equivalent-diameter hollow cylinder (Claesson and Javed 2011; Lamarche and Beauchamp 2007; Salim-Shirazi and Bernier 2013). Such models can be solved in the Laplace domain (Bandyopadhyay et al. 2008; Beier and Smith 2003) or in the time domain (Javed and Claesson 2011; Lamarche 2015; Lamarche and Beauchamp 2007). Another way of accounting for short-term effects, without transforming the geometry into an equivalent diameter, is to use the infinite line source model in a cylindrical composite medium (Li and Lai 2012; Yang and Li 2014). This approach can be used for modeling various types of GHEs, including single and double U-shaped tubes, W-shaped channels, and helical-coils. However, since the infinite line source model does not account for the annual load imbalances, it cannot be used for a long-term thermal processes.

Other authors have investigated the impacts of short-term effects on the borehole length evaluated by the ASHRAE equation. Lamarche (2016) used an alternative model to the ASHRAE equation that uses g-function to determine the ground thermal resistances. He observed that by neglecting the thermal capacity of the boreholes the length is somewhat oversized, especially when the hourly peak ground load is much larger than the monthly ground load. Gagné-Boisvert and Bernier (2016) took into account the thermal capacity inside the borehole and heat pump cycling. Running annual simulations with a TRC model they proposed to multiply the ASHRAE sizing equation by a correction factor. The correction factor can reach 0.69 when oversized heat pumps

operate intermittently and 1.24 for undersized heat pumps and low thermal capacity boreholes.

Li et al. (2017) suggested an alternative to the ASHRAE sizing equation that considers not only the short-term effects but also account for the vertical temperature variation of the fluid inside the U-tubes. The quasi-three-dimensional (3D) model uses a full-scale line source model for heat transfer outside the U-tubes that accounts for the short-term (with the use of the composite medium solution), the mid-term (with the use of the infinite line source solution), the long-term temperature responses, and also the thermal interaction between the boreholes (with the use of the FLS solution). The proposed method is applied to the four test cases introduced by Cullin et al. (2015) and it is shown that the borehole lengths evaluated with their proposed method are closer to the actual lengths and are also shorter than the ones evaluated by the classic ASHRAE sizing equation.

Some authors have argued that the errors in the ASHRAE sizing equation are caused by the use of only three load pulses. For instance, Cullin et al. (2014) compared the sizing ASHRAE equation with GLHEpro in sizing of a 3×2 bore field. The results showed that GLHEpro under predicted the required GHE length by 4% when compared to the actual length, while the ASHRAE sizing method lead to an over prediction of 103%. Later, Cullin et al. (2015) used the same design tool and the ASHRAE sizing equation to evaluate the design lengths of four different systems with operating data. The GLHEpro tool predicted the borehole lengths to within 6% in all four cases, while the ASHRAE sizing equation evaluated lengths with errors ranging from -21% to 167%. The authors explained that most of the error is related to the way that loads are represented in the ASHRAE sizing equation while the differences related to the borehole thermal resistance are less important.

In summary, past studies indicate that the ASHRAE sizing equation has several drawbacks including: (1) the use of the 1D infinite cylinder solution for long time which is inadequate for the long-term effective ground thermal resistances; (2) the inappropriate calculation of the temperature penalty, T_p ; (3) the noninclusion of borehole thermal capacity or variation of the vertical fluid temperature along the U-tubes; (4) the inability of the method to find the maximum length during the first year of operation. In the current article, an alternative to the ASHRAE sizing equation is proposed to alleviate the first three deficiencies. The fourth drawback has been examined by Monzó et al. (2016) and will not be covered in the present article.

The alternative method proposed in the current article has first been introduced by Ahmadfard and Bernier (2014). It is also included in the latest version of the ASHRAE Handbook (ASHRAE 2015) in a separate section entitled "Alternative sizing method." The article expands the analysis provided by Ahmadfard and Bernier (2014) and examines four aspects of this new methodology. First, it is shown that the time-consuming evaluation of the full g-function curve, typically obtained by temporal superposition, is not necessarily required. Second, the optimum number of borehole segments to obtain an accurate bore field length with reasonable calculation time is examined. In addition, the selection

of a convergence criteria and its impact on calculation time is discussed. Finally, the alternative method is modified to account for short-term effects. The proposed alternative method is presented in the next section and is then applied for sizing various bore field configurations and compared to other sizing tools in the following sections.

Modifications to ASHRAE's classic sizing equation

As shown in Equation 3, the alternative method uses the same three pulse methodology as the classic ASHRAE sizing equation.

$$L = \frac{q_a R_{ga,g} + q_m R_{gm,g} + q_h R_{gh,g} + q_h R_b}{T_m - T_g} \quad (3)$$

The three ground pulses, q_a , q_m , and q_h are applied over time periods which are typically equal to 10 years (t_y), 1 month (t_m), and 4 or 6 hours (t_h), respectively. The corresponding ground thermal resistances, $R_{ga,g}$, $R_{gm,g}$, $R_{gd,g}$ are evaluated based on the principle of temporal superposition (ASHRAE 1995, 2015):

$$\begin{aligned} R_{ga,g} &= [g(t_f) - g(t_f - t_1)] / 2\pi k_g \\ R_{gm,g} &= [g(t_f - t_1) - g(t_f - t_2)] / 2\pi k_g \\ R_{gd,g} &= [g(t_f - t_2)] / 2\pi k_g, \end{aligned} \quad (4)$$

where $t_f = t_y + t_m + t_h$, $t_2 = t_y + t_m$ and $t_1 = t_y$. The subscript "g" denotes that the effective ground thermal resistances are evaluated using g-functions. g-Functions account for the thermal interactions among boreholes and the correction provided by the temperature penalty in the classic ASHRAE sizing equation is no longer required. When short-term effects caused by borehole thermal capacity are important, short-term g-functions should be used for the $g(t_f - t_2)$ term which is present in $R_{gm,g}$, $R_{gd,g}$. The determination of short-term g-functions will be addressed later in the current article.

As explained by Bernier (2014), long-term g-functions depend mainly on three nondimensional parameters: r_b/H , B/H , and t/t_s where t_s is the characteristic time ($= H^2/9\alpha$). The main drawback of the proposed alternative method is that an iterative procedure is required because g-functions depend on the length of the borehole which is unknown *a priori*. Most of the current commercially available sizing programs use a pre-stored data base of g-functions with specific r_b/H and B/H ratios. For values of B/H other than the ones associated with the g-functions, logarithmic interpolation between pre-computed g-functions can be used. However, as stated by Malayappan and Spitler (2013), interpolation may result in sizing errors of a few percent. For values of r_b/H different than the ones associated with the g-functions, Eskilson (1987) recommends applying a correction factor but it is also unclear if this correction factor applies to all cases.

For cases where r_b/H and B/H ratios are different, correction factors for r_b/H or interpolation between different B/H curves are required. The method suggested in the article does

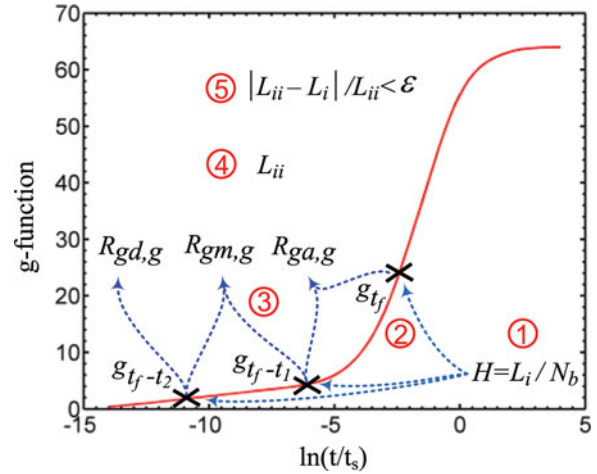


Fig. 2. Illustration of the five-step procedure for the alternative method.

not need to use any correction factors or interpolation as it uses the exact values of r_b/H , B/H and $\ln(t/t_s)$ in each iteration. In addition, the g-function values required at the various time are evaluated independently of previous g-functions as the temporal superposition is not used for the evaluation of g-functions. In this way, g-functions are evaluated dynamically as the calculation to obtain L progresses from iteration to iteration.

Figure 2 shows schematically the five-step iteration procedure of the alternative method. A guess value of $L_i = (N_b \times H_i)$ is first selected. Using this guess value, three g-functions are evaluated based on the proper values of $\ln(t/t_{s,i})$, r_b/H_i and B/H_i . The whole g-function curve does not need to be evaluated since only three g-function values corresponding to three time periods, $t_f - t_2$, $t_f - t_1$ and t_f are required in each iteration. In the third step, the three g-functions are used to calculate the effective ground thermal resistances (Equation 4) which are then used, in step 4, to evaluate the required borehole length L_{ii} (Equation 3). This length L_{ii} is then compared to the guessed or the previous length L_i . If the two lengths agree to within a certain tolerance ϵ , then the solution is said to have converged. If not, the length L_{ii} is then used as the new guess value for the next iteration.

Evaluation of g-functions

The approach suggested by Cimmino and Bernier (2013, 2014) is used to determine g-functions over the full-time scale. This approach can generate g-functions for any bore field geometry. Each borehole is subdivided into a number of segments and the thermal response of every borehole segment is calculated using the FLS analytical solution. Then, spatial superposition is used to calculate the total temperature variation at the borehole wall of every segment. While Cimmino and Bernier (2013, 2014) solved their equation in the Laplace domain, the equations developed here are solved in the time domain.

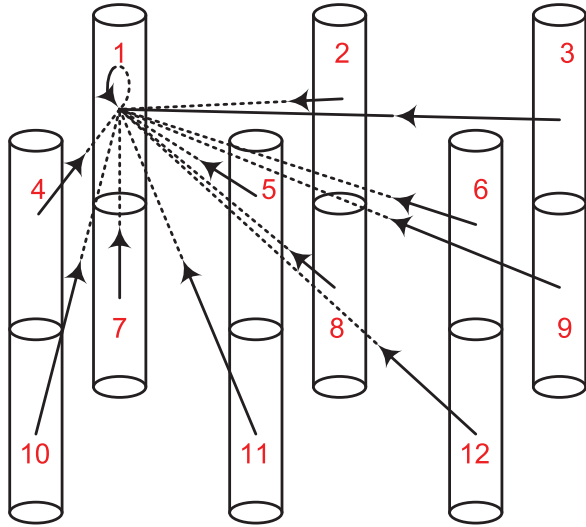


Fig. 3. Schematic illustration of the thermal interaction of all boreholes segments toward segment #1.

The process of generating g-functions is shown in Figure 3 for a 3 × 2 configuration where each borehole is subdivided into two equal length segments ($H_i = H/2$) giving a total of 12 segments. The thermal interactions of all segments toward segment #1, including segment #1 on itself, are illustrated schematically on this figure. In accordance with Eskilson’s definition of the g-function, the borehole wall temperature T_b is the same for every borehole segments in the bore field. This condition is referred to as boundary condition #3 (BC-III) by Cimmino and Bernier (2014). The heat extraction rate per unit length Q_i of each segment is assumed uniform along its length. The total heat extraction rate per unit length \bar{Q} of all boreholes is considered fixed and constant in time. The ground thermal properties are assumed to be isotropic and constant.

In order to evaluate the g-functions for a certain heat extraction rate \bar{Q} at a certain time t_k , the thermal response, $h_{i,j}(t_k)$ among all segments i (1:12) toward each segment j (1:12) need to be calculated. These interactions are evaluated analytically using the FLS following the approach of Cimmino and Bernier (2013):

$$h_{i,j}(t_k) = \frac{1}{2} \int_{1/\sqrt{4\alpha_g t_k}}^{\infty} \exp(-r_{i,j}^2 s^2) \frac{Y(H_s s, D_i s, D_j s)}{H_j s^2} ds, \quad (5)$$

where

$$\begin{aligned} Y(H_s s, D_i s, D_j s) = & f((D_j - D_i + H_s)s) \\ & + f((D_j - D_i - H_s)s) + 2f((D_j + D_i + H_s)s) \\ & - 2f((D_j - D_i)s) \\ & - f((D_j + D_i)s) - f((D_j + D_i + 2H_s)s), \end{aligned}$$

and

$$f(x) = x \cdot \text{erf} x - (1 - \exp(-x^2))/\sqrt{\pi},$$

erf is the error function, H_s are the segment lengths, D_i and D_j are the depths of the borehole segments i and j from the ground surface, and $r_{i,j}$ is the radial distance between segments i and j . Cimmino and Bernier (2013) modified the original approach of Claesson and Javed (2011) to account for various borehole depth and heat extraction rate variation using borehole segments.

The radial distance of segments located in the same borehole is equal to r_b . Thermal response values can be reorganized in a square (12×12 in this example) matrix as follows:

$$\begin{bmatrix} h_{1,1} & h_{2,1} & \cdots & h_{11,1} & h_{12,1} \\ h_{1,2} & h_{2,2} & & h_{11,2} & h_{12,2} \\ \vdots & \vdots & \ddots & \vdots & \vdots \\ h_{1,11} & h_{2,11} & \cdots & h_{11,11} & h_{12,11} \\ h_{1,12} & h_{2,12} & & h_{11,12} & h_{12,12} \end{bmatrix}. \quad (6)$$

Because of symmetry, some terms in this H-matrix are identical ($h_{1,12} = h_{3,10}$, for example). In these cases, the proposed methodology calculates h only once to limit calculation time. The segment-to-segment thermal response factor (Equation 5) needs to be multiplied by the corresponding nondimensional heat extraction rate of each segment. For a typical segment j the following equation is then applied:

$$\begin{aligned} h_{1,j} \tilde{Q}_1(t_k) + h_{2,j} \tilde{Q}_2(t_k) + \cdots + h_{11,j} \tilde{Q}_{11}(t_k) \\ + h_{12,j} \tilde{Q}_{12}(t_k) + \theta_{b,j}^*(t_k) = \theta_b(t_k), \end{aligned} \quad (7)$$

where $\theta_b(t_k)$ is the nondimensional temperature variation at the borehole wall (which is the same for all segments) at time t_k . This value is in fact the g-function. The nondimensional heat extraction rate per unit length of each segment i is given by $\tilde{Q}_i(t_k) (= Q_i(t_k)/\bar{Q})$. The product $h_{i,j} \tilde{Q}_i(t_k)$ accounts for the nondimensional temperature variation at the borehole wall of the j th borehole segment due to the extraction/injection of heat by the i th borehole segment at time t_k . $\theta_{b,j}^*(t_k)$ is a term that accounts for the “history-effect” of the time variation of the heat extraction rates. This term has been determined by Cimmino and Bernier (2013) and can be evaluated with the following expression:

$$\begin{aligned} \theta_{b,j}^*(t_k) = & \left[\sum_{p=1}^{k-1} \sum_{i=1}^{N_b \cdot N_s = 12} h_{i,j}(t_k - t_{p-1}) \tilde{q}_i(t_p) \right] \\ & - h_{i,j}(t_k - t_{k-1}) \tilde{Q}_i(t_{k-1}). \end{aligned} \quad (8)$$

In this equation, $\tilde{q}_i(t_p)$ is equal to $\tilde{Q}_i(t_p) - \tilde{Q}_i(t_{p-1})$, where p is the time step counter. As shown in Equation 8, $\theta_{b,j}^*$ uses temporal superposition. The heat extraction rates and the thermal interactions related to the $k - 1$ previous time steps, are needed to evaluate the g-function at t_k .

In the $N_b \times N_s$ equations (Equation 7), there are $N_b \times N_s$ unknown heat extraction rates, $\tilde{Q}_{i=1:12}$, and one unknown g-function, $\theta_b(t_k)$. The last equation to close the problem

is based on the fact that the total heat extraction rate is constant:

$$\sum_{i=1}^{N_b \cdot N_s} \tilde{Q}_i(t_k) = N_b \cdot N_s \rightarrow \tilde{Q}_1(t_k) + \tilde{Q}_2(t_k) + \dots + \tilde{Q}_{11}(t_k) + \tilde{Q}_{12}(t_k) = 12. \quad (9)$$

Finally, the system of equations can be re-casted in the following matrix form:

$$\begin{bmatrix} h_{1,1} & h_{2,1} & \dots & h_{11,1} & h_{12,1} \\ h_{1,2} & h_{2,2} & & h_{11,2} & h_{12,2} \\ \vdots & & \ddots & \vdots & \\ h_{1,11} & h_{2,11} & \dots & h_{11,11} & h_{12,11} \\ h_{1,12} & h_{2,12} & \dots & h_{11,12} & h_{12,12} \\ 1 & 1 & \dots & 1 & 1 \end{bmatrix} \begin{bmatrix} -1 \\ -1 \\ \vdots \\ -1 \\ -1 \\ 0 \end{bmatrix} \times \begin{bmatrix} \tilde{Q}_1(t_k) \\ \tilde{Q}_2(t_k) \\ \vdots \\ \tilde{Q}_{11}(t_k) \\ \tilde{Q}_{12}(t_k) \\ \theta_b(t_k) \end{bmatrix} = \begin{bmatrix} \theta_{b,1}^* \\ \theta_{b,2}^* \\ \vdots \\ \theta_{b,11}^* \\ \theta_{b,12}^* \\ N_b \cdot N_s = 12 \end{bmatrix} \quad (10)$$

By solving this system of equations, the 12 heat extractions $\tilde{Q}_i(t_k)$ as well as the g-function $\theta_b(t_k)$ are obtained at time t_k . Equation 10 is the resulting system of equations for the 3×2 configuration with 2 segments per borehole. As can be expected, calculation time increases significantly with an increase in the number of boreholes and borehole segments. In addition, as will be shown later, asymmetric bore fields also lead to long calculation times.

As shown later in the article, the evaluation of $\theta_{b,j}^*$ can potentially be neglected for bore field sizing purposes. Consequently, g-functions can be evaluated without considering temporal superposition of heat extraction rates at previous time steps. Thus, the value of the heat extraction rates of all segments as well as the g-functions are evaluated directly at time t_k . As will be shown below, the generation of g-functions without temporal superposition reduces computational time significantly which is an important aspect of the proposed alternative method since g-functions are evaluated several times in the iterative process.

It should be pointed out that the methodology that is described here for the evaluation of g-functions is not specific to the ASHRAE sizing equation but can be used whenever g-functions are required.

Neglecting temporal superposition when generating g-function values

Bore field sizing using the proposed alternative method (Equation 3) requires g-function at three time values on the g-function curve (Figure 2) for each iteration. Typically, as shown below, 3 to 5 iterations are required. Thus, 9 to 15 g-function values are required to size a bore field. There are several ways to obtain these g-function values. First, as noted

in the introduction, pre-calculated g-function curves can be used. However, these are typically valid for fixed values of B/H and r_b/H . It is possible to interpolate between B/H curves and correct for various r_b/H ratio but with a lost in accuracy which is difficult to quantify.

Second, one can generate the entire g-function curve for the exact B/H and r_b/H ratios by solving Equation 10 at several times, t_k . Temporal superposition is used to account for the “history-effect” of the time variation of the heat extraction rates of the borehole segments. Then, the three g-function values would be obtained by interpolation on the g-function curve. This process would have to be repeated three to five times depending on the number of iterations. Cimmino and Bernier (2013) evaluated the entire curve based on 71 individual values of t_k . They used time steps of one hour for the first 48 hours and then they doubled the time step for each subsequent time to cover the full time span of the g-function curve. In the present work, the same technique is employed but with 19 individual values of t_k evaluated at times corresponding to $\ln(t/t_s) = -14, -13, \dots, 3, 4$. This accelerates the evaluation of the g-functions curve when compared to the technique of Cimmino and Bernier (2013). In sizing problems discussed later in the article that are solved with temporal superposition, 19 g-functions values are calculated in each iteration and then the three g-functions are interpolated from these values.

The third method which is even faster and is the one recommended here, is to calculate the g-function directly at the required value of $\ln(t_k/t_s)$ without temporal superposition. Thus, the $\theta_{b,j}^*(t_k)$ term in Equation 10 is considered to be equal to zero. Until now most researchers used temporal superposition to obtain g-functions (e.g., Cimmino and Bernier 2013). However, as shown later in the current article, this is not necessary.

The accuracy of a direct calculation of the g-function without temporal superposition will now be evaluated for several bore field configurations. The first configuration to be studied is a 12×10 bore field with $H = 100$ m, $D = 4$ m, $r_b = 75$ mm and $B = 6.5$ m. The g-functions are calculated with 12 equal-length segments. Figure 4a shows g-function curves evaluated using the three techniques just described with the bottom graph showing the relative difference between the technique without temporal superposition and two methods with temporal superposition where the entire g-function curve is generated with either 19 or 71 points. The maximum relative difference of the results is approximately 2.9% (with the 71-point curve) and occurs at a value of $\ln(t/t_s) \approx -1$ where the g-function curve has its steepest slope. As shown on the top scale, this value corresponds to a time of 15 years for a 100 m borehole and a ground thermal diffusivity of $0.075 \text{ m}^2/\text{day}$. If this borehole is to be sized for a 10- to 20-year period, then the value of $R_{ga,g}$ will be the one most affected by this difference. However, as will be shown later in the article, the overall effect of this difference on bore field length is minimum since the $R_{ga,g}$ term is typically not the dominant term in Equation 3.

Figure 4b shows three series of curves. The upper and lower curves show, respectively, the time variation of $\sum_{p=1}^{k-1} \sum_{i=1}^{N_b \cdot N_s = 12} h_{i,j}(t_k - t_{p-1}) \tilde{q}_i(t_p)$ and of $-h_{i,j}(t_k - t_{k-1}) \tilde{Q}_i(t_{k-1})$ for all segments. The summation of these values

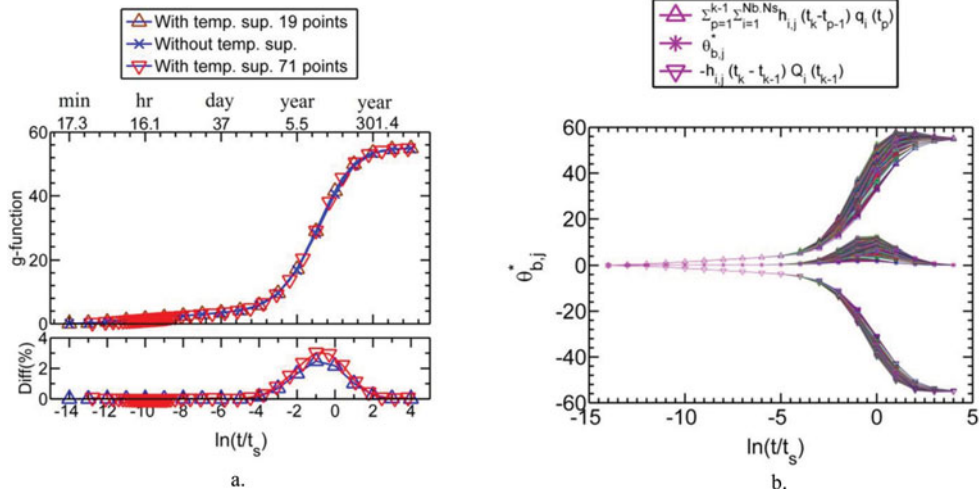


Fig. 4. a. g-Function curves determined with and without the temporal superposition and their relative difference; b. Variation of θ_b^* as a function of nondimensional time.

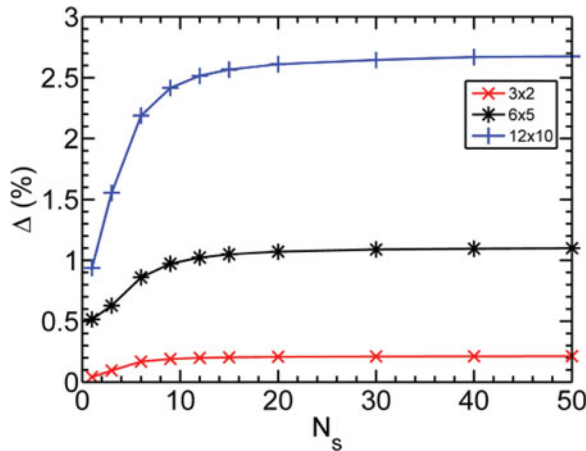


Fig. 5. The effect of the number of segments and number of boreholes on Δ , the maximum difference between g-functions evaluated with and without temporal superposition.

is equal to $\theta_{b,j}^*$, represented by the middle curves. As expected, the values of $\theta_{b,j}^* \neq 0$ for $\ln(t/t_s) \approx -1$ which explains the difference observed in the g-function value in Figure 4a.

Figure 5 presents the maximum relative difference of the g-functions obtained with temporal superposition for 19 t_k values and the ones that are evaluated without temporal superposition as a function of the number of segments. In addition to the 12 x 10 configuration, the comparisons are done for two other configurations of 6 x 5 and 3 x 2 boreholes. For each of these cases, the input parameters are the same as those used for Figure 4.

These results show that the maximum difference, typically occurring at $\ln(t/t_s) \approx -1$, between the two methods increases with the number of boreholes. This is due to increased thermal interactions between boreholes that cause greater time variations of the heat extraction rates. The maximum difference also increases with the number of segments

up to a certain point around 12 to 15 segments where the maximum difference stabilizes.

Verification of the proposed alternative method

The previous section examined the impact of calculating g-functions without temporal superposition. This section looks more closely at the accuracy of the proposed method for sizing of vertical GHEs. Therefore, the methodology is first compared with other sizing tools for six different borehole configurations. Then, the effects of temporal superposition, number of borehole segments, convergence criteria, and initial guesses are evaluated separately for a typical sizing problem. Finally, the effects of these parameters and also the effect of bore field symmetry on the calculation time and the boreholes overall length are discussed for two borehole configurations.

Ground loads and input parameters used in the comparisons

The ground load profile used in the current article is presented in Figure 6 where negative loads indicate that the building is in heating mode and that the GHX collects heat from the ground. The same annual load is repeated for a 10-year cycle.

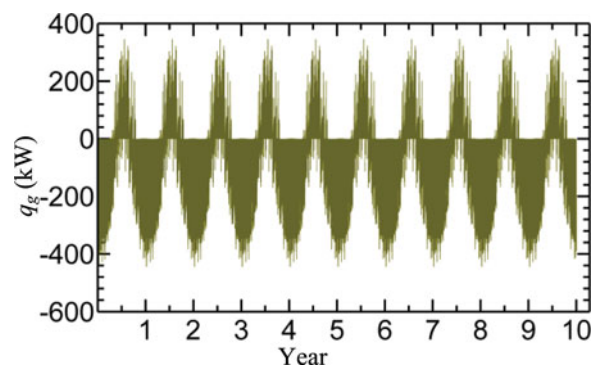


Fig. 6. Ground loads used in the comparison cases.

Table 1. Monthly average and peak ground loads in cooling and heating.

	Jan.	Feb.	Mar.	Apr.	May	Jun.	Jul.	Aug.	Sept.	Oct.	Nov.	Dec
q_m (kW)	-146.4	-144.7	-123.0	-74.5	-17.6	31.0	41.9	30.6	-14.5	-62.3	-98.1	-136.0
$q_{h,C}$ (kW)	0.0	0.0	0.0	30.5	225.1	304.4	345.5	323.1	231.5	201.4	0.0	0.0
$q_{h,H}$ (kW)	-443.9	-428.0	-362.4	-309.2	-186.2	-108.9	-70.2	-170.1	-228.1	-297.2	-383.7	-415.8

It is an unbalanced load which causes the ground to get progressively cooler from year to year.

Table 1 provides a monthly summary of this load profile. The average ground loads of each month, q_m , are evaluated based on the average of all hourly loads of that month including the two heating and cooling peaks, $q_{h,C}$ and $q_{h,H}$, occurring during that month. Considering that the largest peak heating load (-443.9 kW) is larger than the largest peak cooling load (345.5 kW), and that there is a negative thermal imbalance, the required bore field length will be determined when the building is in peak heating mode. Therefore, only the required bore field length in heating will be evaluated here. Corresponding ground loads to be used for three pulse methods are presented in Table 2.

The borehole parameters and ground properties used in the following analysis are reported in Table 3. It should be noted that the minimum entering fluid temperature limit, T_L and the undisturbed ground temperature are set to 0°C and 18°C, respectively.

These loads are used for six different borehole configurations which are shown on the first row in Table 4.

With the conditions presented in Table 3 and with the ground load profile given in Figure 6, 120 boreholes (12 × 10) each with a length of approximately 100 m are required. This configuration represents the base case (5th column in Table 4). Other test cases, with a lower or larger number of boreholes, use a load profile which is proportional to the number of boreholes. Hence, a geometry with 25 boreholes will have values of q_a , q_m , and q_h which correspond to 25/120 times the value presented in Tables 1 and 2. Sizing with the proposed method is performed using three thermal pulses with $t_y = 10$ years, $t_m = 1$ month, and $t_h = 6$ hours.

Comparison with other sizing methods

In the current section, the proposed method is compared with four other sizing tools/methods. These methods will be described briefly. None of these methods account for short-term effects caused by borehole thermal capacity. These effects will be discussed later in the article.

Table 2. Annual, monthly, and hourly ground loads used by the three pulse methods.

Ground loads	(kW)
q_h	-443.9
q_m	-146.4
q_a	-59.0

The commercial sizing tool called Earth Energy Designer (EED; Blomberg et al. 2015) uses a data base of pre-calculated g-functions to size bore fields. The program interpolates between g-function values by keeping the borehole spacing constant but changing borehole depth. The data base includes g-functions for the in-line, L, U, O and

Table 3. Borehole parameters and ground thermal properties.

Parameter	Value
Ground	
Ground thermal conductivity (k_g)	1.8 W/(m.K)
Ground thermal diffusivity (α_g)	0.075 m ² /day
Undisturbed ground temperature (T_g)	18°C
Bore field	
Borehole buried depth (D)	4 m
Borehole spacing (B)	6.5 m
Borehole	
Borehole radius (r_b)	75 mm
Number of pipes	2
Pipe outer radius ($r_{p,out}$)	16.7 mm
Pipe inner radius ($r_{p,in}$)	13 mm
Center to center distance between pipes (d_p)	62 mm
Pipe thermal conductivity (k_p)	0.4 W/(m.K)
Pipe volumetric heat capacity	1540 kJ/(K.m ³)
Grout thermal conductivity (k_{gr})	1 W/(m.K)
Grout volumetric heat capacity	3900 kJ/(K.m ³)
Contact resistance (R_c)	0 W/(m.K)
Resulting borehole thermal resistance (R_b)	0.20 m.K/W
Fluid	
Fluid viscosity (μ_f)	0.00179 kg/(m.s)
Fluid density (ρ_f)	1016 kg/m ³
Fluid specific heat capacity (C)	4000 J/(kg.K)
Fluid thermal conductivity (k_f)	0.513 W/(m.K)
Fluid flow rate (\dot{m})	0.043 kg/s per kW of peak load
Minimum entering fluid temperature limit (T_L)	0°C
Convection coefficient (h_{conv})	1000 W/(m ² .K)

Table 4. Comparison between the proposed method and four other sizing tool.

	19: (9,1,9)	25: (1 × 25)	28: (9,1,8,1, 9)	36: (8,1,8,1,8,1,8,1)	120: (12 × 10)	127: Axisymmetric
Bore field geometry	Borehole length (m) (Percentage difference relative to the proposed method without temporal superposition)					
Proposed method without temporal superposition	77.0	76.8	77.6	78.9	106.1	112.6
Proposed method with temporal superposition	77.1 (0.1)	76.9 (0.1)	77.7 (0.1)	80.0 (0.1)	107.4 (1.2)	114.1 (1.3)
EED	79.8 (3.7)	77.4 (0.9)	77.2 (0.5)	78.1 (1.0)	111.6 (5.2)	—
Classic ASHRAE equation with T_p from Fossa and Rolando (2013)	78.9 (2.6)	78.7 (2.6)	79.5 (2.6)	80.9 (2.5)	108.6 (2.3)	115.2 (2.3)
Classic ASHRAE equation with T_p from Bernier et al. (2008)	79.6 (3.4)	79.4 (3.4)	80.2 (3.4)	81.5 (3.4)	109.1 (2.8)	115.7 (2.7)
DST-GenOpt	—	—	—	—	—	120.6 (7.1)

rectangular geometries. Thus, it cannot size the axisymmetric configuration shown in the last column of Table 4. EED requires user-defined average monthly heating and cooling loads and peak heating and cooling loads to determine the average and the peak monthly mean fluid temperatures. Peak heat loads are added to the average heat loads at the end of each month. It also assumes that the peak heat loads do not have any influence on the long-term behavior as they are already considered in the average load.

The next two sizing methods use the ASHRAE sizing equation but with better evaluations of the temperature penalties based on the methodologies suggested by Bernier et al. (2008) and Fossa and Rolando (2013). As mentioned previously, Bernier et al. (2008) suggest to evaluate the temperature penalties T_p using $Q_u(g_{N_b} - g_1)/(2\pi k_g N_b H)$, while Fossa and Rolando (2013) suggest a slightly different method where T_p is equal to $Q_u(g_{N_b}/2\pi - G)/(k_g N_b H)$. The value of Q_u in these equations is the unbalanced load which is equal to $(q_a t_y + q_m t_m + q_h t_h)/(t_y + t_m + t_h)$.

The last sizing method uses the Duct ground STORAGE (DST) model in the TRNSYS environment as explained by Ahmadfard et al. (2016). The DST model is typically used for a known borehole length; it is not a sizing tool. However, when combined with GenOpt it is possible to find the optimum (i.e., minimum) borehole length such that the outlet temperature from the bore field is within the temperature limits, T_L and T_H . For each iteration, GenOpt makes a new guess for the borehole length and then it calls the DST model to do a multi-year simulation. The objective functions as well as the optimization design parameters are the same as the ones used by Ahmadfard et al. (2016). The DST model is strictly valid for an axisymmetric configuration which explains the

choice of the configuration shown in the last column in Table 4.

For the results reported in Table 4, the g-functions used in the proposed method and for the evaluation of the temperature penalties are calculated with twelve segments. The reported temperature penalties and borehole lengths are evaluated iteratively with the use of a convergence criterion of 0.1% and an initial guess for the borehole length of 100 m.

Results obtained by the proposed method with and without temporal superposition are very close to each other (within 0.1%) for nondense bore fields but show slightly higher differences (1.2% to 1.3%) for denser bore fields. This is not as high as the maximum difference, around 2.5%, shown in Figure 5 for 120 boreholes. This is due to the fact that the maximum difference in the g-function only affects the $q_a R_{ga,g}$ term in the sizing equation. This impact is presented in Table 5 where it is shown that the difference between g-functions evaluated with and without temporal superposition does not affect the short time periods and so the monthly and hourly effective ground thermal resistances of the two models are identical. Therefore, the main difference is related to the yearly ground thermal resistances. For nondense bore fields, the difference in the value of $R_{ga,g}$ is small but for denser bore fields the difference is in-line with the values shown in Figure 5. For example, the difference in the value of $R_{ga,g}$ for the 120-borehole configuration in Table 5 is around 3%. However, this does not translate into a 3% difference in the bore field length as $R_{ga,g}$ is multiplied by q_a in the sizing equation (Equation 3). Thus, depending on the weight of the $q_a R_{ga,g}$ term in Equation 3, the impact of the difference between g-functions evaluated with and without temporal superposition will be more or less significant. In the case reported in

Table 5. Comparison of the three ground thermal resistances evaluated with and without temporal superposition.

	Without temporal superposition		With temporal superposition	
Bore field geometry	19: (9,1,9)	120: (12 × 10)	19: (9,1,9)	120: (12 × 10)
Length (m)	77.0	106.1	77.1	107.4
$R_{gh,g}$ (m.K/W)	0.092	0.092	0.092	0.092
$R_{gm,g}$ (m.K/W)	0.209	0.209	0.209	0.209
$R_{ga,g}$ (m.K/W)	0.555	1.789	0.560	1.844
Calculation time (s)	36	50	240	486

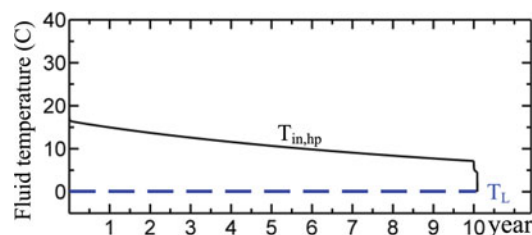
Table 4, the overall difference on the length is of the order of 1.2% to 1.3%. Finally, the last line in Table 5 shows that calculation times with temporal superposition are seven to ten times longer than without temporal superposition.

The results evaluated without temporal superposition and the ones obtained using EED with the monthly pulses are in good agreement except for the L and rectangular bore field configurations where the differences are 3.7% and 5.2%. As shown previously, only 1.2% of this difference is related to the error associated with the generation of g-functions without temporal superposition. The remaining difference might be attributed to different modeling approaches.

Table 6 presents the results of a comparison between EED and the two proposed models with and without temporal superposition. In this comparison, the annual ground heat load is assumed to be zero. The results are obtained using 1 and 12 segments for the evaluation of the g-function. It can be seen that all methods lead to the same length of 63.9 m. This tends to demonstrate that when there is no annual ground thermal imbalance, the proposed method can be used with one segment and without temporal superposition. The calculation times in the last column in Table 6 show that it is clearly advantageous to reduce the number of segments and to perform the calculations without temporal superposition.

Results presented in Table 4 also show that the borehole lengths obtained using the ASHRAE equation compare favorably well with other methods if the temperature penalties are evaluated properly. This is in contrast with the work of Cullin et al. (2015) who reported that the classic ASHRAE sizing equation evaluated with the original temperature penalty method showed differences ranging from -21% to 167% when compared to four different systems with operating data.

The last row of Table 4 is related to the result of the DST-GenOpt tool for an axisymmetric configuration. The difference between this method and the proposed method without temporal superposition is 7.1%. Sizing with the DST-GenOpt approach is achieved within the TRNSYS environment using hourly time steps in order to mimic the three pulse approach. Hence, the hourly ground load contains 87600 hours at -59.0 kW, 744 hours at -146.4 kW and 6 hours at -443.9 kW. Figure 7 shows the evolution of the outlet fluid temperature from the bore field for the last iteration of the DST-GenOpt approach. As can be seen, the outlet

**Fig. 7.** Evolution of the outlet fluid temperature for the last iteration of the DST-GenOpt method.

temperature from the bore field decreases steadily for the first 10 years, then there are two sudden downward steps associated with the monthly and hourly pulses before the fluid temperature reaches a value of 0°C, the minimum temperature limit.

Finally, it should be mentioned that based on the results reported in Table 4, the proposed method has, on average, a 2.9% difference with the other four sizing methods.

Convergence criteria, initial guess values and number of segments

The proposed method is iterative in nature and results depend on the convergence criteria and initial guess values. The impact of these two factors are examined for the 12 × 10 sizing problem presented earlier with three different convergence criteria of 0.01%, 0.1%, and 1% and with two initial guess values for the borehole length, 50 and 200 m. Table 7 presents the results of this analysis which was obtained without temporal superposition and with 12 borehole segments. As expected, stricter convergence criteria leads to more iterations and longer calculation times. However, the evaluated lengths do not vary significantly. A 0.1% convergence criteria, for example, a 0.1 m error for a 100 m borehole, appears to be a good compromise between accuracy and calculation time. Results also show that the alternative method converges to the same value whether the initial guess is significantly lower (50 m) or higher (200 m) than the final length.

The impact of the number of borehole segments is analyzed using the same 12 × 10 geometry by varying the number of segments from 1 to 25 and using 0.1% convergence criteria. This problem is solved with and without temporal superposition and results are shown in Figures 8a and 8b. As

Table 6. Comparison of several methods when there is no annual ground thermal imbalance.

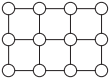
Configuration	Method	Number of segments	Number of iterations	Length (m)	Calculation time (s)
	Proposed method without temporal superposition	1	2	63.9	1.1
		12	2	63.9	34.7
	Proposed method with temporal superposition	1	2	63.9	5.1
		12	2	63.9	270.6
	EED	—	—	63.9	1.0

Table 7. Analysis of the effects of various convergence criteria and initial guess values on the results.

Convergence criteria, ϵ (%)	Initial guessed length (m)	Number of iterations	Final length (m)	Calculation time (s)
1	50/200	3/3	106/106	52.9/52.8
0.1	50/200	4/4	106.1/106.1	70.9/70.0
0.01	50/200	5/5	106.07/106.07	87.6/87.4

can be seen, the results obtained with and without temporal superposition follow the same pattern; the relative differences in length between 1 and 25 segments are 3.4% and 4% with and without temporal superposition. The calculation time in both cases increases exponentially with the number of borehole segments. However, the calculation times obtained without temporal superposition are significantly shorter than the ones obtained using temporal superposition. For example, for 1 segment, the calculation times are 8 and 3.1s with and without temporal superposition, respectively. The corresponding number for 25 segments are 2081 and 213s. These results are obtained on a computer equipped with an Intel core i5 processor (2.70 GHz) and 8 GB of RAM. Twelve borehole segments appear to be a good compromise between

accuracy and calculation time in line with the findings of Cimmino and Bernier (2014).

It has also been observed that the optimum number of borehole segments is slightly dependent on the borehole length. For example, for the same geometry (12 × 10), if the loads are doubled, the resulting borehole length evaluated without temporal superposition is 197.8 m for one segment and 193.3 m for 25 segments, a 2.3% difference. If the loads are reduced in half, the resulting borehole length is 55.3 m for one segment and 52.3 m for 25 segments, a 5.7% difference. Thus, it appears that fewer segments could be used for longer boreholes. This is due to the fact that borehole end effects are proportionally less significant for longer boreholes. This fact can be used to

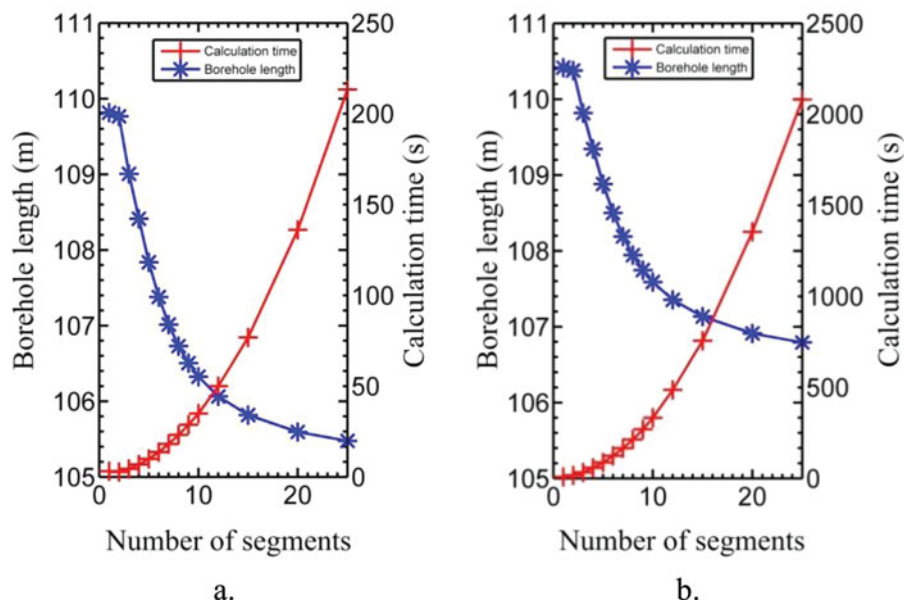


Fig. 8. Borehole length and corresponding calculation time as a function of the number of segments obtained a. without; and b. with temporal superposition.

reduce the calculation time of the proposed method. However, as the length of the boreholes is not known at the beginning of the iterations, the number of segments should be optimized during iterations. For example, only one segment could be used in the first iteration and then the number of segments could be increased/decreased in the next iterations based on the evaluated borehole lengths.

The effect of symmetry on calculation time

As a final point regarding calculation time, it is interesting to examine a bore field composed of randomly placed boreholes with no symmetry. This was done using a bore field composed of 120 boreholes which are scattered arbitrarily in an $80 \times 80 \text{ m}^2$ ground area with a minimum borehole separation of 6.5 m. The ground heat load and the input parameters are identical to those reported in Tables 2 and 3. This problem is solved with convergence criteria of 0.1% using 12 segments with and without temporal superposition with corresponding calculation times of 34,070 and 5169s which are, respectively, about 70 and 100 times longer than the ones for rectangular equally spaced 12×10 bore field (486 and 50s). Thus, symmetry plays a major role in the reduction of calculation time.

Short-term effects

It is possible to account for short-term effects associated with borehole thermal capacity using the same sizing equations (Equations 3 and 4) with so-called short-term g-functions. The method used here to evaluate short-term g-functions is based on the work of Xu and Spitler (2006) which finds its origin in the method proposed by Yavuzturk and Spitler (1999). Xu and Spitler (2006) approximated the U-tube geometry with a series of hollow cylinders representing the fluid, the fluid convective resistance, the pipe, the grout and the ground. The outer diameter of the equivalent pipe is simply taken as the square root of two multiplied by the outer diameter of the pipe. An equivalent grout thermal conductivity is used based on the determination of the grout thermal resistance obtained from the multipole method. Radial heat transfer from the fluid to the ground is then solved numerically to obtain g-functions using the definition given by Yavuzturk and Spitler (1999). Xu and Spitler (2006) have shown that results obtained with this technique compare favorably well with the ones obtained with a 2D model representing the real borehole geometry.

In the current article, the only modification to the Xu and Spitler (2006) approach is that heat transfer from the borehole wall to the ground is calculated using the ICS solution. The required heat transfer rate at the borehole wall is obtained from the numerical solution and the borehole wall temperature boundary condition required by the numerical model is calculated from the ICS solution.

Figure 9 shows the short-time g-function curve obtained for the borehole described in Table 3. The g-function curve without short-term effects (for a 12×10 bore field) is also shown in this figure. The two curves merge into the same curve after a certain time ($\ln(t/t_s) \approx -8$ in the case of Figure 9). As shown on Figure 9, g-functions are lower when short-term

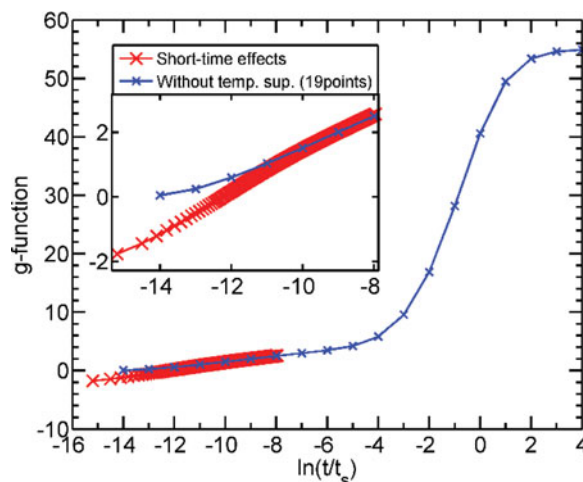


Fig. 9. g-functions obtained with and without short-term effects for a 12×10 bore field.

effects are considered. Short-term g-functions are independent of borehole length and spacing as well as bore field configuration. Therefore, the evaluated g-functions (illustrated in Figure 9) can be used for any bore field configurations, as long as the parameters are identical to the ones specified in Table 3.

To show the impact of short time effects on the borehole lengths, results presented in Table 4 are recalculated using short-time g-functions for the $g_{(t_f-t_2)}$ term (see Equation 4). The monthly and yearly g-functions are calculated using the long-term g-functions based on 12 segment boreholes and without using temporal superposition. As shown in Table 8, the resulting boreholes are shorter by about 2.8% to 3.9% when short-term effects are considered. This is to be expected as borehole thermal capacity will dampen the change in the borehole wall temperature following a change in the amount of heat injected into a borehole. These differences are similar to the ones obtained by Lamarche (2016).

The differences presented in Table 8 are problem dependent and cannot be generalized. In order to further examine these differences the values of the effective ground thermal resistances (Equation 4) are presented in Table 9 for the 12×10 geometry for peak durations of 1 and 6 hours. As shown in this table, there are significant differences in the values of $R_{gd,g}$ and $R_{gm,g}$. For example, for the 6-hour peak duration, $R_{gd,g}$ decreases from 0.092 to 0.068 m.K/W while $R_{gm,g}$ increases from 0.209 to 0.233 m.K/W. These differences are mainly due to the fact that short-term g-functions are slightly lower than the ones evaluated without short-term effects. The value of $R_{ga,g}$ changes slightly but in this case the variation is not due to short-term effects but to the fact that the borehole length has changed (due to short-term effects) which in turn changes the value of the long-term g-function. These changes in the three effective ground thermal resistances reduce the required borehole length by 3.0%. This difference is dependent on the relative strengths of q_a , q_m , and q_h . Generally, when the value of q_h increases when compared to q_a and q_m , then the difference in the required

Table 8. Comparison of borehole lengths obtained with and without short time effects.

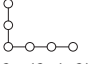
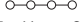

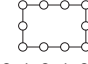
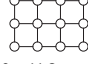

Bore field geometry	 19: (9,1,9)	 25: (1 × 25)	 28: (9,1,8,1, 9)	 36: (8,1,8,1,8,1,8,1)	 120: (12 × 10)	 127: Axisymmetric
With short time effects (m)	74.0	73.8	74.6	75.9	102.9	109.5
Without short time effects (m)	77.0	76.8	77.6	78.9	106.1	112.6
Relative difference	-3.9%	-3.9%	-3.9%	-3.8%	-3.0%	-2.8%

Table 9. The effects of short time effects and peak duration on the boreholes lengths of 12 × 10 bore field

Peak duration Short term effects	6 hours		1 hour	
	Without short term effects	With short term effects	Without short term effects	With short term effects
Length (m)	106.1	102.9	97.6	88.6
Relative difference		-3.0%		-9.2%
$R_{gh,g}$ (m.K/W)	0.092	0.068	0.028	-0.039
$R_{gm,g}$ (m.K/W)	0.209	0.233	0.273	0.340
$R_{ga,g}$ (m.K/W)	1.789	1.777	1.754	1.711
$R_b + R_{gh,g}$ (m.K/W)	0.292	0.268	0.228	0.161

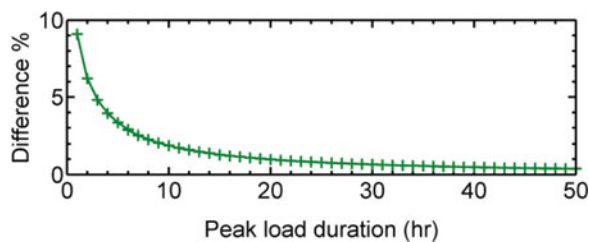


Fig. 10. Relative length difference with and without short-term effects.

borehole length with and without short-term effects will increase.

When the peak duration is only 1 hour, the required borehole length when the short-term effects are considered is 9.2% shorter than when short-term effects are not considered. As noted in Table 9, $R_{gh,g}$ is negative for a 1-hour peak duration, however, the sum $R_b + R_{gh,g}$ is positive.

In addition to peak durations of 1 and 6 hours, the same sizing problem has been checked with peak durations ranging from one hour to 50 hours and the results are shown in Figure 10. It can be shown that length differences with and without short-term effects are negligible after 50 hours for this configuration and load pattern.

Conclusions

This study proposes modifications to the ASHRAE sizing equation for vertical GHEs. The resultant method uses the same three pulse methodology as the classic ASHRAE sizing equation. The three effective ground thermal resistances corresponding to the three heat pulses are evaluated with the

use of three g-functions. Since g-functions evaluate the thermal interactions between the boreholes, there is no need to consider the “temperature penalty” present in the ASHRAE sizing equation. However, an iterative procedure is required as g-functions depend on the borehole length that is unknown *a priori*. One important aspect of the iterative procedure is that it is able to evaluate new g-functions dynamically as the solution progresses. Approximately 3 to 5 iterations are required to obtain a converged solution, thus the proposed methodology requires the evaluation of 9 to 15 single g-function values. These values are evaluated analytically using the FLS by discretizing boreholes in axial segments and without applying any interpolation on the g-function curve or between pre-determined g-functions. In addition, contrary to previous works, temporal superposition is not used for evaluating the g-functions as results show that it does not have a significant effect on the boreholes length. However, it affects the calculation time noticeably. For example, for a 12 × 10 bore field sized with 12 segments, the lengths evaluated with and without temporal superposition have a 1.2% relative difference. However, calculation time is about 10 times longer with temporal superposition. It is also seen that longer boreholes need fewer borehole segments. This is due the fact that the boreholes end effects are proportionally less significant for longer boreholes. It is also concluded that convergence criteria of 0.1% (0.1 m on a 100 m borehole) gives sufficiently accurate results with reasonable calculation time. The proposed methodology is compared against four other sizing methods including EED, the DST model of TRNSYS combined with GenOpt and the classic ASHRAE equation with appropriate temperature penalty calculations. Six different borehole configurations ranging from a 19 borehole L-shape bore field to a 127 axisymmetric configuration are used in this comparison. The average relative difference

between the results of the proposed method and the other sizing methods is 2.9%. Finally, it is shown that short-term g-functions can be used to account for borehole thermal capacity in the proposed method. Short-term effects have an impact on the hourly and monthly effective ground thermal resistances. In one particular case studied here, the required length is 3.0% shorter when short-term effects are considered for a 6-hour peak duration. When the peak duration is reduced to 1 hour, this difference increases to 9.2%.

Funding

This work was performed under a discovery grant provided by the Natural Sciences and Engineering Research Council of Canada (NSERC).

References

- Ahmadfard, M., and M. Bernier. 2014. An alternative to ASHRAE's design length equation for sizing borehole heat exchangers. *ASHRAE Annual Conference, Seattle, USA, July 1, paper SE-14-C049, 8 pages.*
- Ahmadfard, M., M. Bernier, and M. Kummert. 2016. Evaluation of the design length of vertical geothermal boreholes using annual simulations combined with Genopt. *Proceedings of eSim Building Performance Simulation Conference, May 3–6, McMaster University, Hamilton, Ontario, Canada, pp. 46–57.*
- ASHRAE. 1995. *Chapter 32—Geothermal Energy. ASHRAE Handbook—Applications.* Atlanta: ASHRAE.
- ASHRAE. 2015. *Chapter 34—Geothermal Energy, ASHRAE Handbook—Applications,* Atlanta: ASHRAE.
- Bandyopadhyay, G., W. Gosnold, and M. Mann. 2008. Analytical and semi-analytical solutions for short-time transient response ground heat exchangers. *Energy and Buildings* 40(10):1816–24.
- Beier, R., and M. Smith. 2003. Minimum duration of in-situ tests on vertical boreholes. *ASHRAE Transactions* 109(2): 475–86.
- Bernier, M. 2006. Closed-loop ground-coupled heat pump systems. *ASHRAE Journal* 48(9):12–9.
- Bernier, M. 2014. Sizing and simulating bore fields using thermal response factors. *Proceedings of the 11th IEA Heat Pump conference, Montreal (Quebec), Canada, May 2014. Paper KN.3.1.1.*
- Bernier, M.A., A. Chahla, and P. Pinel. 2008. Long-term ground-temperature changes in geo-exchange systems. *ASHRAE Transactions* 114(2):342–50.
- Blomberg, T., J. Claesson, P. Eskilson, G. Hellström, and B. Sanner. 2015. EED v3.2—Earth Energy Designer. *User Manual,* BLOCON, Lund, Sweden.
- Bose, J.E., J.D. Parker, and F.C. McQuiston. 1985. *Design/Data Manual for Closed-Loop Ground-Coupled Heat Pump Systems.* Atlanta: ASHRAE.
- Capozza, A., M. De Carli, and A. Zarrella. 2012. Design of borehole heat exchangers for ground-source heat pumps: A literature review, methodology comparison and analysis on the penalty temperature. *Energy and Buildings* 55:369–79.
- Cimmino, M., and M. Bernier. 2013. Preprocessor for the generation of g-functions used in the simulation of geothermal systems. *Proceedings of the 13th International IBPSA Conference, Chambéry, France, August 25–30, pp. 2675–82.*
- Cimmino, M., and M. Bernier. 2014. A semi-analytical method to generate g-functions for geothermal bore fields. *International Journal of Heat and Mass Transfer* 70:641–50.
- Claesson, J., and S. Javed. 2011. An analytical method to calculate borehole fluid temperatures for time-scales from minutes to decades. *ASHRAE Transaction* 117:279–88.
- Cullin, J.R., C. Montagud, F. Ruiz-Calvo, and J.D. Spitler. 2014. Experimental validation of ground heat exchanger design methodologies using real, monitored data. *ASHRAE Transactions* 120:357–69.
- Cullin, J.R., J.D. Spitler, C. Montagud, F. Ruiz-Calvo, S.J. Rees, S.S. Naicker, P. Konečný, and L.E. Southard. 2015. Validation of vertical ground heat exchanger design methodologies. *Science and Technology for the Built Environment* 21(2):137–49.
- Eskilson, P. 1987. Thermal analysis of heat extraction boreholes. Doctoral Thesis, Department of Mathematical Physics, University of Lund, Lund, Sweden.
- Fossa, M. 2011. The temperature penalty approach to the design of borehole heat exchangers for heat pump applications. *Energy and Buildings* 43(6):1473–9.
- Fossa, M., and D. Rolando. 2013. An improved method for vertical geothermal borefield design using the temperature penalty approach. *European Geothermal Congress (EGC), pp. 1–8.*
- Fossa, M., and D. Rolando. 2015. Improving the ASHRAE method for vertical geothermal bore field design. *Energy and Buildings* 93: 315–23.
- Fossa, M., and D. Rolando. 2016. Improved ASHRAE method for BHE field design at 10 year horizon. *Energy and Buildings* 116:114–21.
- Gagné-Boisvert, L., and M. Bernier. 2016. Accounting for borehole thermal capacity when designing vertical geothermal heat exchangers. *ASHRAE Summer Conference, St-Louis, Missouri, June 2016. Paper ST-16-C027.*
- Hellström, G., and B. Sanner. 2000. *Earth Energy Designer. User's Manual, version 2.*
- Javed, S., and J. Claesson. 2011. New analytical and numerical solutions for the short-term analysis of vertical ground heat exchangers. *ASHRAE Transaction* 117(1):3–12.
- Kavanaugh, S.P. 1995. A design method for commercial ground-coupled heat pumps. *ASHRAE Transactions* 101(2):25–31.
- Lamarche, L. 2015. Short-time analysis of vertical boreholes, new analytical solutions and choice of equivalent radius. *International Journal of Heat and Mass Transfer* 91:800–7.
- Lamarche, L. 2016. Short-time modelling of geothermal systems. *Proceedings of ECOS 2016, June 19–23, Portoroz, Slovenia. 9 pages.*
- Lamarche, L., and B. Beauchamp. 2007. New solutions for the short-time analysis of geothermal vertical boreholes. *International Journal of Heat and Mass Transfer* 50:1408–19.
- Li, M., and A. Lai. 2012. New temperature response functions (G functions) for pile and borehole ground heat exchangers based on composite-medium line-source theory. *Energy* 38:255–63.
- Li, M., and A.C.K. Lai. 2015. Review of analytical models for heat transfer by vertical ground heat exchangers (GHES): A perspective of time and space scales. *Applied Energy* 151:178–91.
- Li, M., X. Zhuo, and G. Huang. 2017. Improvements on the American Society of Heating, Refrigeration, and Air-Conditioning Engineers Handbook equations for sizing borehole ground heat exchangers. *Science and Technology for the Built Environment* 23(8):1267–1281.
- Malayappan, V., and J.D. Spitler. 2013. Limitations of using uniform heat flux assumptions in sizing vertical borehole heat exchanger fields. *Proceedings of Clima 2013, Prague, Czech Republic, June 16–19.*
- Monzó, P., M. Bernier, J. Acuna, and P. Mogensen. 2016. A monthly-based bore field sizing methodology with applications to optimum borehole spacing. *ASHRAE Transactions* 122:111–26.
- Pasquier, P., and D. Marcotte. 2012. Short-term simulation of ground heat exchanger with an improved TRCM. *Renewable Energy* 46: 92–9.
- Philippe, M., M. Bernier, and D. Marchio. 2009. Validity ranges of three analytical solutions to heat transfer in the vicinity of single boreholes. *Geothermics* 38(4):407–13.
- Philippe, M., M. Bernier, and D. Marchio. 2010. Sizing calculation spreadsheet: Vertical geothermal borefields. *ASHRAE Journal* 52(7):20–8.

- Ruiz-Calvo, F., M. De Rosa, J. Acuña, J.M. Corberan, and C. Montagud. 2015. Experimental validation of a short-term borehole-to-ground (B2G) dynamic model. *Applied Energy* 140: 210–23.
- Salim-Shirazi, A., and M. Bernier. 2013. Thermal capacity effects in borehole ground heat exchangers. *Energy and Buildings* 67:352–64.
- Spitler, J.D., and M. Bernier. 2016. *Advances in ground-source heat pump systems—Chapter 2: Vertical borehole ground heat exchanger design methods*. S. Rees, ed. Duxford, UK: Woodhead (Elsevier) Publishing, pp. 29–61.
- Spitler, J.D. 2000. GLHEPRO—A design tool for commercial building ground loop heat exchangers. *Proceedings of the Fourth International Heat Pumps in Cold Climates Conference*, Aylmer, Québec, August 17–18.
- Xu, X., and J.D. Spitler. 2006. Modeling of vertical ground loop heat exchangers with variable convective resistance and thermal mass of the fluid. *Proceedings of the 10th International Conference on Thermal Energy Storage—Ecostock 2006*, Pomona, NJ, May 31–June 2.
- Yang, Y., and M. Li. 2014. Short-time performance of composite-medium line-source model for predicting responses of ground heat exchangers with single U shaped tube. *International Journal of Thermal Sciences* 82:130–7.
- Yavuzturk, C., and J.D. Spitler. 1999. A short time step response factor model for vertical ground loop heat exchangers. *ASHRAE Transactions* 105:475–85.
- Zarrella, A., M. Scarpa, and M. De Carli. 2011. Short time step analysis of vertical ground coupled heat exchangers: The approach of CaRM. *Renewable Energy* 36(9):2357–67.